OPEN ACCESS
OPUS AUGSBURG

Universität Augsburg
Universitätsbibliothek

Covering a broad dynamic range: information processing at the erythropoietin receptor

Verena Becker, Marcel Schilling, Julie Bachmann, Ute Baumann, Andreas Raue, Thomas Maiwald, Jens Timmer, Ursula Klingmüller

Angaben zur Veröffentlichung / Publication details:

Becker, Verena, Marcel Schilling, Julie Bachmann, Ute Baumann, Andreas Raue, Thomas Maiwald, Jens Timmer, and Ursula Klingmüller. 2010. "Covering a broad dynamic range: information processing at the erythropoietin receptor." Science 328 (5984): 1404–8. https://doi.org/10.1126/science.1184913.

Nutzungsbedingungen / Terms of use: **licgercopyright**

Dieses Dokument wird unter folgenden Bedingungen zur Verfügung gestellt: / This document is made available under these conditions:
Deutsches Urheberrecht
Weitere Informationen finden Sie unter: / For more information see:
https://www.uni-augsburg.de/de/organisation/bibliothek/publizieren-zitieren-archivieren/publiz/

Covering a Broad Dynamic Range: Information Processing at the Erythropoietin Receptor

Verena Becker,[1,2]* Marcel Schilling,[1]* Julie Bachmann,[1] Ute Baumann,[1] Andreas Raue,[3] Thomas Maiwald,[3]† Jens Timmer,[3,4,5] Ursula Klingmüller[1,2]‡

Cell surface receptors convert extracellular cues into receptor activation, thereby triggering intracellular signaling networks and controlling cellular decisions. A major unresolved issue is the identification of receptor properties that critically determine processing of ligand-encoded information. We show by mathematical modeling of quantitative data and experimental validation that rapid ligand depletion and replenishment of the cell surface receptor are characteristic features of the erythropoietin (Epo) receptor (EpoR). The amount of Epo-EpoR complexes and EpoR activation integrated over time corresponds linearly to ligand input; this process is carried out over a broad range of ligand concentrations. This relation depends solely on EpoR turnover independent of ligand binding, which suggests an essential role of large intracellular receptor pools. These receptor properties enable the system to cope with basal and acute demand in the hematopoietic system.

Cells respond to alterations in their environment that are frequently encoded by changes in the concentration of extracellular ligands. These changes are perceived by cell surface receptors, and the high frequency with which receptors are mutated in diseases and their accessibility to drugs make them key targets for therapeutic interventions. The dynamics of receptor activation are critically determined by the capacity to capture and sequester ligand through endocytosis (*1*). Ligand-encoded information could be processed in a saturation-like or linear mode for increasing ligand concentrations (Fig. 1A). Receptor properties enabling cells to cope with ligand concentrations that vary over a broad range remained to be identified.

A prime example for a receptor that encounters an extreme range of ligand concentrations is the erythropoietin receptor (EpoR). The EpoR ensures continuous renewal of short-lived erythrocytes (*2*) and enhanced expansion of erythroid progenitors upon demands such as blood loss. Plasma concentrations of erythropoietin (Epo) can differ ~1000-fold between basal and acute conditions (*3*). Only a small proportion of EpoR is present on the cell surface; the majority resides in intracellular pools (*4*). Ligand binding triggers phosphorylation of the cytoplasmic EpoR domain by Janus kinase 2 (JAK2) (*5*). Ligand-induced endocytosis of EpoR has been proposed to terminate signaling by removing receptors from the cell surface (*6*). Additionally, the EpoR is subjected to ligand-independent endocytosis (*7*) [supporting online material (SOM) text]. The specific impact of EpoR transport to the plasma membrane and EpoR endocytosis on processing of ligand-encoded information have remained ill-defined.

Linear detection of ligand over a broad range of concentrations could be facilitated by the following properties reported for other receptors (Fig. 1, B to D, and SOM text): (i) mobilization, defined as ligand-induced additional transport of newly synthesized receptor from intracellular pools to the plasma membrane (*8*); (ii) recycling, consisting of ligand-induced receptor endocytosis and subsequent transport back to the plasma membrane (*9*); and (iii) turnover, comprising ligand-independent transport of newly synthesized receptor to the plasma membrane and removal from the plasma membrane by ligand-

[1]Division Systems Biology of Signal Transduction, DKFZ-ZMBH Alliance, German Cancer Research Center, 69120 Heidelberg, Germany. [2]Bioquant, Heidelberg University, 69120 Heidelberg, Germany. [3]Institute of Physics, University of Freiburg, 79104 Freiburg, Germany. [4]Freiburg Institute for Advanced Studies, University of Freiburg, 79104 Freiburg, Germany. [5]Centre for Biological Signalling Studies (BIOSS), University of Freiburg, 79104 Freiburg, Germany.

*These authors contributed equally to this work.
†Present address: Department of Systems Biology, Harvard Medical School, Boston, MA 02115, USA.
‡To whom correspondence should be addressed. E-mail: u.klingmueller@dkfz-heidelberg.de

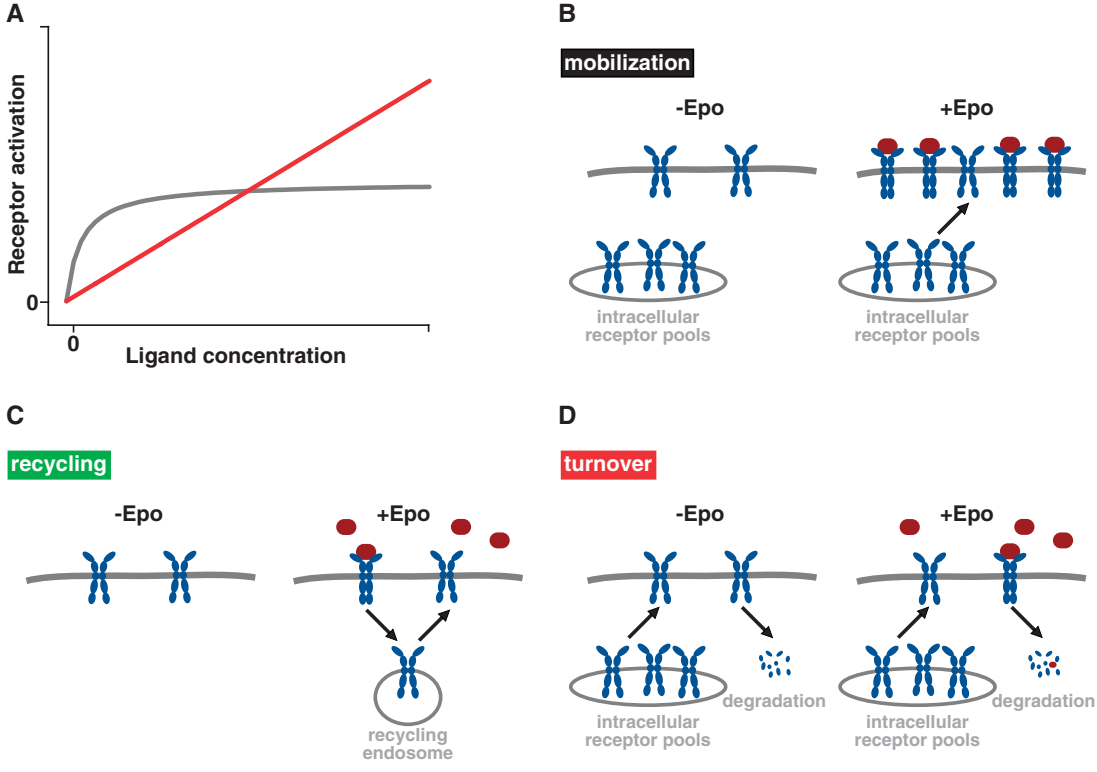

Fig. 1. Strategies of information processing through cell surface receptors for a broad range of ligand concentrations. (**A**) Representation of two modes for information processing. (**B** to **D**) Hypothetical mechanisms for linear information processing through the EpoR: mobilization, recycling, and turnover (see text).

independent receptor endocytosis and subsequent degradation (*10*). A further potential strategy to cope with particularly high ligand concentrations is expression of large amounts of receptor on the plasma membrane (*11*). However, the abundance of EpoR on the cell surface is rather low (*12*) (fig. S1 and SOM text).

Receptor mobilization, recycling, and turnover are highly dynamic and intertwined processes that are difficult to disentangle experimentally. To address these nonlinear processes, we developed dynamic mathematical models for ligand-receptor interaction and trafficking kinetics and fitted them to quantitative experimental data (*13*). The core model included parameters for EpoR recycling and turnover (Fig. 2A) and was compared with an extended model encompassing receptor mobilization (core model + k_{mob}) (fig. S5A). Briefly, unoccupied cell surface EpoR is subjected to turnover with transport of newly synthesized receptor to the plasma membrane ($k_t \times B_{max}$)—where B_{max} is the maximal binding capacity of the total cell surface receptor population—and ligand-independent endocytosis (k_t). Epo binds to cell surface receptor with the association rate k_{on} and dissociates with the rate k_{off}. The definition of the parameter k_{off} is based on the dissociation constant K_D ($k_{on} \times K_D$). Epo-EpoR complexes are subjected to endocytosis (k_e). These complexes dissociate, and EpoR and Epo recycle back to the plasma membrane (k_{ex}) or undergo degradation. Degraded Epo is retained in intracellular compartments (k_{di}) or released to the extracellular space in an inactive state (k_{de}), unable to rebind to EpoR. In our extended model, we additionally integrated EpoR mobilization as a single parameter k_{mob} to summarize its overall effect, including a chaperone action mediated by the protein kinase JAK2 (*14*) (fig. S2A).

We calibrated the mathematical model on the basis of experimental data from BaF3-EpoR cells, a murine proB cell line that exogenously

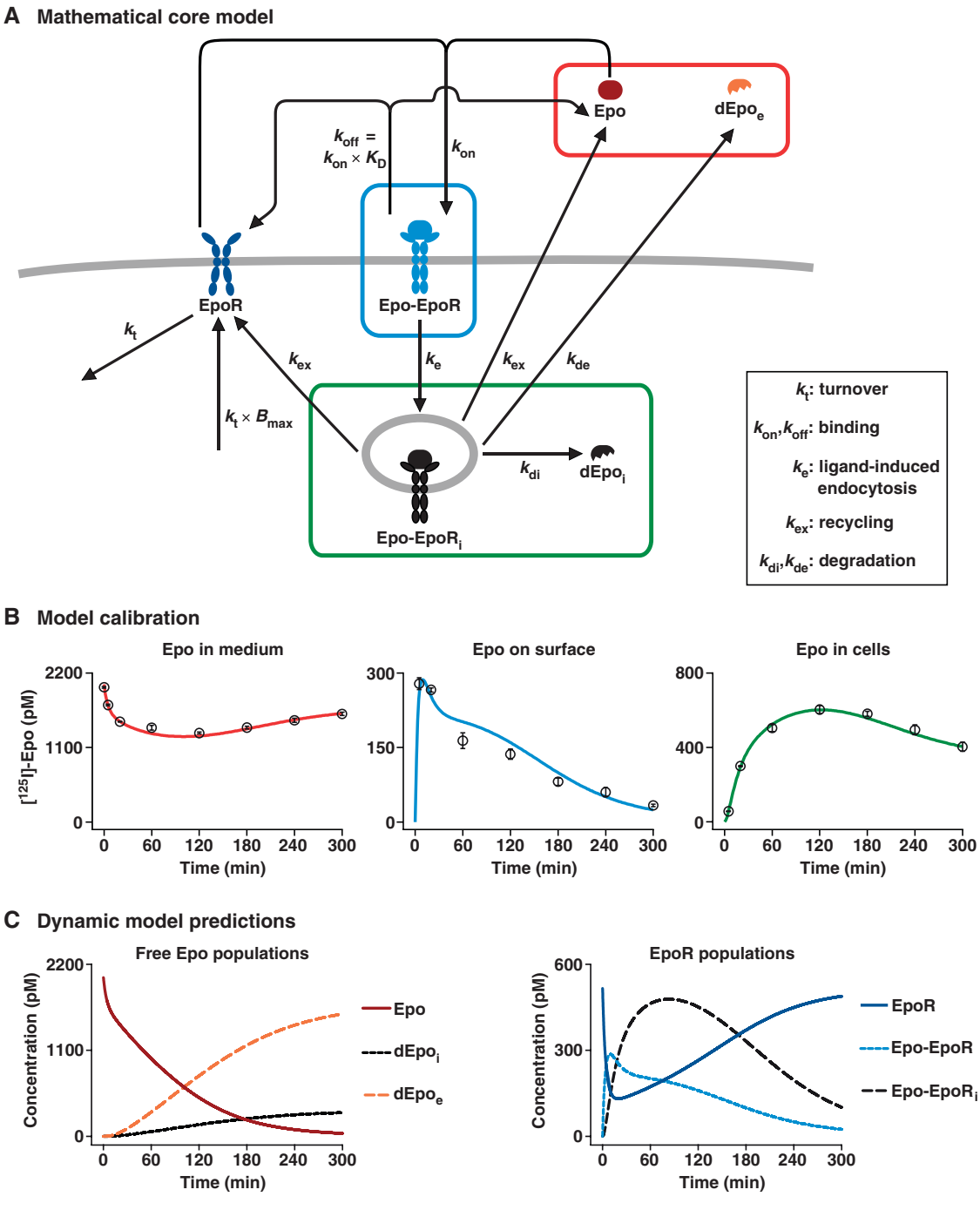

Fig. 2. Dynamic modeling of the EpoR system. (**A**) Graphical representation of the mathematical core model. Colored boxes indicate the experimentally accessible quantities "Epo in medium" (Epo + dEpo$_e$, red), "Epo on surface" (Epo-EpoR, blue), and "Epo in cells" (Epo-EpoR$_i$ + dEpo$_i$, green). Biological processes described by individual reaction rates are given in the inset. (**B**) Global parameter estimation was performed simultaneously for the core model and the auxiliary model (fig. S4). Experimental data for the core model are represented with standard deviations ($n = 3$), and trajectories of the best fit are shown. (**C**) Trajectories for the predicted behavior of experimentally unobserved dynamic variables of the core model.

expresses EpoR. The parameters B_{max} and K_D were measured using ^{125}I-labeled Epo (*13*) (fig. S1). To determine the rate k_t, we built an analog auxiliary model for EpoR turnover (fig. S2B), using a streptavidin-binding peptide (SBP)–tagged EpoR (fig. S3 and SOM text). The kinetics of radiolabeled ligand was monitored (fig. S3D), and we estimated parameters simultaneously for the core model and the auxiliary model (*15*). The trajectories of the best fit captured the observed dynamics (Fig. 2B and fig. S4A). The underlying models were minimal models that were both consistent with biological knowledge and well determined by the experimental data. Each calibrated model is structurally and practically identifiable within tight confidence intervals as shown by the likelihood profile (*16*) (fig. S4B). Comparing the contributions of reactions describing transport of EpoR from intracellular pools to the plasma membrane for the extended core model + k_{mob} revealed that the flux $k_{mob} \times$ Epo-EpoR is more than one order of magnitude lower than the flux $k_t \times B_{max}$ and therefore negligible (fig. S5B). Furthermore, the performance of the extended model was lower than that of the core model as revealed by statistical tests (fig. S5C). Therefore, EpoR mobilization is unlikely to make a major contribution, and further analyses focused on the core model to determine the impact of receptor recycling and turnover.

The calibrated core model enabled us to predict key dynamic properties of the EpoR system (fig. S6). The ratio of the rate for EpoR turnover ($k_t = 0.033\ min^{-1}$) to the rate for ligand-induced endocytosis ($k_e = 0.075\ min^{-1}$) indicated that Epo binding accelerates receptor endocytosis by a factor of about 2. In contrast to the epidermal growth factor receptor (*17*, *18*), this low ratio implies a less prominent contribution of ligand-induced EpoR removal from the plasma membrane to attenuate receptor activity (SOM text). Model simulations for species not directly accessible by experimental measurements predicted that intact Epo is rapidly depleted from the medium by endocytosis-mediated uptake and subsequent degradation (Fig. 2C, left, and SOM text). Unoccupied EpoR on the plasma membrane was predicted not to diminish by more than 75% of the maximal value B_{max} and to recover almost entirely (Fig. 2C, right). Therefore, the EpoR system never reaches an absolute refractory state but remains continuously ligand-sensitive. To assess dynamic properties that determine conversion of ligand binding into receptor activation, we derived from the model (*13*) the time-dependent half-life of species in a specific subcompartment (fig. S7 and SOM text). This analysis suggested that ligand-induced endocytosis has an important role in shaping the early-response kinetics of EpoR activation.

To confirm experimentally the predicted recovery of cell surface EpoR, we performed time-course analysis of receptor activation in BaF3-EpoR cells. Receptor phosphorylation returned to basal amounts between 60 and 120 min after cells were exposed to Epo (Fig. 3A). However, restimulation of these cells with an excess of ligand resulted in receptor phosphorylation comparable to that after initial activation. In line with model predictions, endocytic removal of cell surface EpoR does not attenuate long-term receptor signaling, but cells remain Epo-responsive. For experimental validation of the model-predicted ligand depletion, BaF3-EpoR cells were treated with Epo, and the culture medium was used as the stimulating medium for another cell pool. The later the medium was collected, the less the receptor was phosphorylated on the treated cells (Fig. 3B). This decrease in stimulating capacity of the medium did not occur in the absence of EpoR (fig. S8A). By determining Epo amounts in the medium, rapid ligand depletion was also directly validated for murine and human EpoR in BaF3 cells, as well as for erythroid progenitors, which showed that receptor-mediated ligand degradation is a general attribute of the EpoR system (fig. S8, B to D, and SOM text). The dynamics of cell surface receptor recovery and ligand depletion challenge the conventional view that EpoR degradation through the proteasome and lysosome (*6*) is a major cause of attenuation of receptor activation. Rapid ligand depletion and receptor recovery for the related interleukin 3 receptor (fig. S9 and SOM text) suggest that these processes are key properties conserved among hematopoietic cytokine receptors.

Model simulations for increasing ligand concentrations showed saturation for the peak amplitude of cell surface Epo-EpoR complexes (Fig. 4A, middle) that resulted from the limited amount of receptor present on the plasma membrane at a given time. A linear relation for integral EpoR occupancy representing the amount of cell surface Epo-EpoR complexes integrated over time was predicted even for high concentrations of Epo (Fig. 4A, right). Measurements of the peak amplitude of phosphorylated EpoR and JAK2 (figs. S10 and S11) coincided with the behavior predicted by model simulations for cell surface Epo-EpoR complexes (Fig. 4B, middle). The linear relation of ligand input and integral EpoR occupancy correlates with the amount of EpoR and JAK2 phosphorylation integrated over time (Fig. 4B, right), which shows that the extracellular stimulus is accurately converted into receptor activation. To discriminate between the influence of receptor recycling and turnover, we performed simulations for various values of the respective parameters. Despite changing the recycling rate k_{ex}, the linear relation of ligand input and integral EpoR occupancy was maintained, but with a different slope (Fig. 4C). The linearity of this relation strictly depended on the turnover k_t (Fig. 4D), which enables cells to constantly repopulate the plasma membrane with newly synthesized receptor from intracellular pools. Although higher k_t rates beyond the estimated value had no impact, with lower turnover rate values, the linear resolution of ligand-encoded information processing in the model gradually decreased. Thus, EpoR turnover at a high rate functions as a linear signal integrator and thus assigns an essential role to large intracellular receptor pools (figs. S12 and S13 and SOM text) and enables cells to detect ligand concentrations that vary over a broad range.

In this study, we identified rapid ligand depletion and compensation of endocytic removal of cell surface EpoR by receptor turnover as hallmarks of the EpoR that facilitate linear information processing for a broad range of ligand concentrations. These systems properties enable cells to sample extracellular ligand continuously and there-

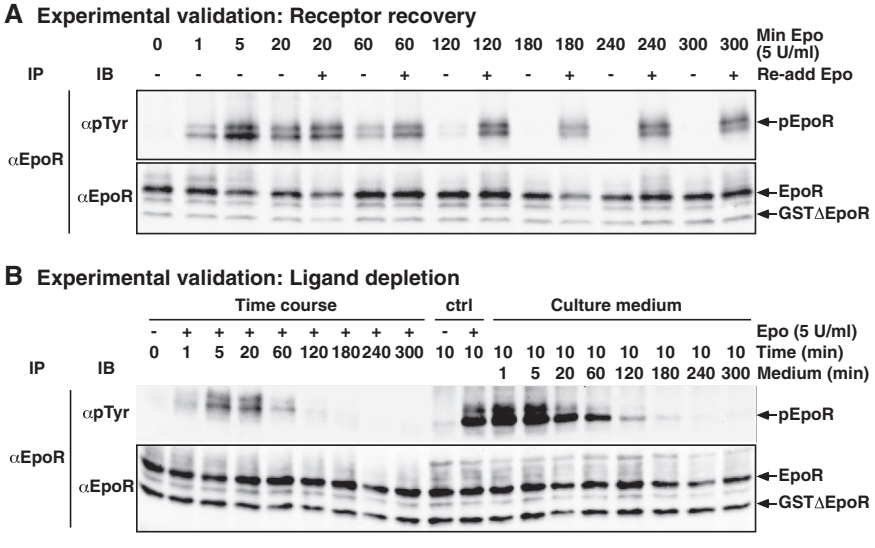

Fig. 3. Experimental validation of model predictions for rapid receptor recovery and ligand depletion. Immunoprecipitates (IP) were analyzed by quantitative immunoblotting (IB) with antibodies against phosphotyrosine (pTyr) and against EpoR. (**A**) BaF3-EpoR cells were stimulated with 5 U/ml Epo, and if indicated, 50 U/ml Epo was added 10 min before cell lysis. (**B**) BaF3-EpoR cells were stimulated with Epo (time course). Freshly starved cells were stimulated for 10 min with culture medium collected at the indicated times (medium) or with Epo (ctrl). pEpoR, phosphorylated EpoR; GST-ΔEpoR, recombinant glutathione *S*-transferase (GST)–tagged protein used as reference.

by to cope with both basal and acute demand-driven ligand concentrations. Epo has been widely applied to treat anemia (*19*), and current research focuses on engineering more efficient erythropoiesis-stimulating agents (*20*). Model simulations for various ligand-binding rates point to a parameter region that displays a trade-off between bioavailability and bioactivity of Epo derivatives (figs. S14 to S16 and SOM text). Thus, the combination of mathematical modeling and quantitative biochemical analysis enables a more rational development of therapeutic agents.

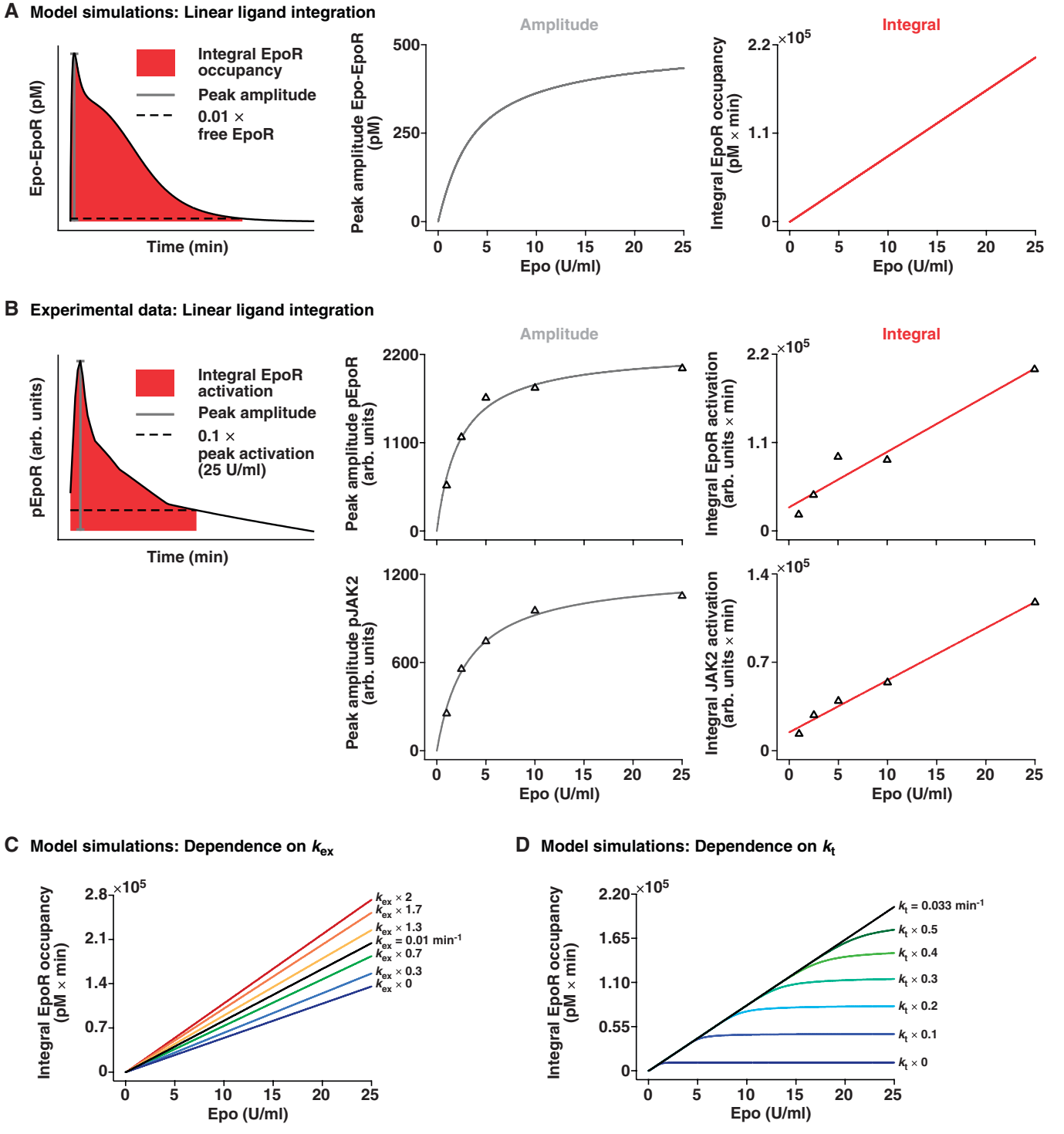

Fig. 4. Linear conversion of Epo concentrations into integral receptor occupancy depends on EpoR turnover. (**A**) Simulations for peak amplitude of Epo-EpoR complexes at the plasma membrane (middle) and integral EpoR occupancy defined as the amount of cell surface Epo-EpoR complexes integrated over time relative to their dependence on Epo (right). Graphical representations are shown for peak amplitude and integral EpoR occupancy (left). (**B**) Experimental data (triangles) were acquired by quantitative immunoblot analysis of EpoR and JAK2 activation in BaF3-EpoR cells (figs. S10 and S11). A Michaelis-Menten–like saturation and a linear function were fitted to the data for peak amplitude (middle) and integral EpoR and JAK2 activation, defined as the amount of phosphorylated protein integrated over time (right), respectively. Graphical representations are shown for peak amplitude and integral EpoR activation (left). (**C** and **D**) Simulations for integral EpoR occupancy for various parameter values around the estimated rates of (C) recycling k_{ex} or (D) turnover k_t. Details for calculating the integral are provided in the SOM text. pEpoR and pJAK2, phosphorylated proteins.

References and Notes

1. H. Shankaran, H. Resat, H. S. Wiley, *PLOS Comput. Biol.* **3**, e101 (2007).
2. H. Wu, X. Liu, R. Jaenisch, H. F. Lodish, *Cell* **83**, 59 (1995).
3. W. Jelkmann, *Intern. Med.* **43**, 649 (2004).
4. A. Yoshimura, A. D. D'Andrea, H. F. Lodish, *Proc. Natl. Acad. Sci. U.S.A.* **87**, 4139 (1990).
5. T. D. Richmond, M. Chohan, D. L. Barber, *Trends Cell Biol.* **15**, 146 (2005).
6. P. Walrafen *et al*., *Blood* **105**, 600 (2005).
7. D. L. Beckman, L. L. Lin, M. E. Quinones, G. D. Longmore, *Blood* **94**, 2667 (1999).
8. K. S. Price *et al*., *Am. J. Respir. Cell Mol. Biol.* **28**, 420 (2003).
9. Z. Bajzer, A. C. Myers, S. Vuk-Pavlović, *J. Biol. Chem.* **264**, 13623 (1989).
10. S. Belouzard, D. Delcroix, Y. Rouillé, *J. Biol. Chem.* **279**, 28499 (2004).
11. G. Carpenter, S. Cohen, *Annu. Rev. Biochem.* **48**, 193 (1979).
12. H. Youssoufian, G. Longmore, D. Neumann, A. Yoshimura, H. F. Lodish, *Blood* **81**, 2223 (1993).
13. Materials and methods are available as supporting material on *Science* Online.
14. L. J. Huang, S. N. Constantinescu, H. F. Lodish, *Mol. Cell* **8**, 1327 (2001).
15. T. Maiwald, J. Timmer, *Bioinformatics* **24**, 2037 (2008).
16. A. Raue *et al*., *Bioinformatics* **25**, 1923 (2009).
17. H. Resat, J. A. Ewald, D. A. Dixon, H. S. Wiley, *Biophys. J.* **85**, 730 (2003).
18. H. S. Wiley *et al*., *J. Biol. Chem.* **266**, 11083 (1991).
19. W. Jelkmann, *Eur. J. Haematol.* **78**, 183 (2007).
20. I. C. Macdougall, K. U. Eckardt, *Lancet* **368**, 947 (2006).

21. We thank R. Eils, U. Kummer, R. Meyer, A. C. Pfeifer, J. P. Schlöder, C. Schultz, and V. Starkuviene for critically reading the manuscript; S. N. Constantinescu for HA-EpoR constructs; and S. Manthey and S. Lattermann for technical assistance. This work was supported by the Helmholtz Alliance on Systems Biology (SBCancer) (V.B., M.S., J.T., and U.K.), the German Federal Ministry of Education and Research (BMBF)–funded MedSys-Network LungSys (J.B., A.R., and U.K.), and the Excellence Initiative of the German Federal and State Governments (EXC 294) (J.T.).

Supporting Online Material

www.sciencemag.org/cgi/content/full/science.1184913/DC1
Materials and Methods
SOM Text
Figs. S1 to S16
References

10.1126/science.1184913